Physica C: Superconductivity and its applications 539 (2017) 13–18

Contents lists available at ScienceDirect

Physica C: Superconductivity and its applications

journal homepage: www.elsevier.com/locate/physc

Effect of template post-annealing on Y(Dy)BaCuO nucleation on CeO_2 buffered metallic tapes

Xuefeng Hu[a], Yun Zhong[b], Huaxiao Zhong[a], Feng Fan[a], Lina Sang[a], Mengyao Li[a], Qiang Fang[a], Jiahui Zheng[a], Haoyu Song[a], Yuming Lu[a], Zhiyong Liu[a], Chuanyi Bai[a], Yanqun Guo[a], Chuanbing Cai[a,*]

[a] Shanghai Key Laboratory of High Temperature Superconductors, Physics Department, 99 Shangda Road, Shanghai University, Shanghai 200444, China
[b] Engineering and Technical Training Center, 99 Shangda Road, Shanghai University, Shanghai 200444, China

ARTICLE INFO

Article history:
Received 28 January 2017
Revised 20 May 2017
Accepted 16 June 2017
Available online 17 June 2017

Keywords:
Ceria buffers
Annealing and post-annealing
Humid Ar/5%H_2
Nucleation
Coated conductor

ABSTRACT

Substrate engineering is very significant in the synthesis of the high-temperature superconductor (HTS) coated conductor. Here we design and synthesize several distinct and stable Cerium oxide (CeO_2) surface reconstructions which are used to grow epitaxial films of the HTS $YBa_2Cu_3O_{7-\delta}$ (YBCO). To identify the influence of annealing and post-annealing surroundings on the nature of nucleation centers, including Ar/5%H_2, humid Ar/5%H_2 and O_2 in high temperature annealing process, we study the well-controlled structure, surface morphology, crystal constants and surface redox processes of the ceria buffers by using X-ray diffraction (XRD), X-ray photoelectron spectroscopy (XPS) and field-emission scanning electronic microscopy (FE-SEM), respectively. The ceria film post-annealed under humid Ar/5%H_2 gas shows the best buffer layer properties. Furthermore, the film absorbs more oxygen ions, which appears to contribute to oxygenation of superconductor film. The film is well-suited for ceria model studies as well as a perfect substitute for CeO_2 bulk material.

1. Introduction

The second-generation (2 G) high-temperature superconductor $REBa_2Cu_3O_{7-\delta}$ (REBCO, RE=Y and Gd, Dy etc rare earths) coated conductors (CCs) wires have now entered into the marketplace reproducibility. However, the current density of long-length 2 G wire production still needs to be better optimized [1–3]. In order to improve the critical current density of YBCO, various techniques have been developed, including improving grain connectivity, introducing high density nano-size defects, and increasing effective superconducting thickness. Besides, superconducting properties of REBCO are significantly affected by surface morphology and crystallinity of buffer layer. It has been found that CeO_2 is a most important material in heterogeneous catalysis due to its high oxygen storage capacity (OSC) based on the oxidation and reduction of cerium ions [4,5]. It is reported that CeO_2 has large oxygen storage capacity because oxygen vacancy defects(CeO_{2-x}) can be rapidly formed and eliminated [6]. And the cubic fluorite structure of CeO_2 is also great interesting due to its outstanding properties such as wide band gap, high thermal and chemical stability, high dielectric constant and unique optical properties, making CeO_2 films a promising material for various applications, such as buffer layers gate dielectric, fuel cells [7–9], sunscreen cosmetics [10], catalysis [11] and ultraviolet blocking filter [12–16]. CeO_2 has been successfully used as cap buffer layer for preventing the interdiffusion and enhancing the compatibility between REBCO and the metallic substrate, for its small lattice mismatch with REBCO, chemical tenability, self-assembling crystalline structure. Usually the structure and nuclei density of YBCO are influenced by the well defined substrate characteristics and processing conditions. Many methods have been used to optimize CeO_2 cap layers, such as UV light irradiation, better synthesize parameters, rare earth doping and post-annealing. Post-annealing is a simple and promising route to optimize the quality of CeO_2. However, there are few reports on post-annealing of CeO_2 under various atmosphere. In this work, we mainly investigate the influence of post-annealing under different processing atmospheres on CeO_2 buffers as well as the subsequent superconducting Y(Dy)BCO layers prepared by metal organic deposition.

2. Experimental

Nano-crystalline CeO_2 thin films around 40 nm are grown on long-length IBAD tape: un-textured Hastelloy alloy metal tape

* Corresponding author.
E-mail addresses: huxuef001@163.com (X. Hu), cbcai@t.shu.edu.cn (C. Cai).

http://dx.doi.org/10.1016/j.physc.2017.06.001
0921-4534/

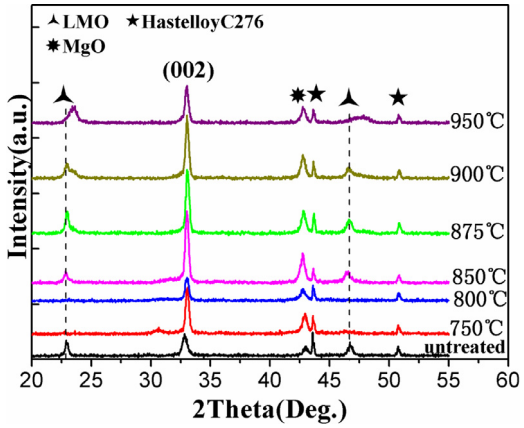

Fig. 1. X-ray $\theta-2\theta$ diffraction patterns of post-annealed CeO_2 films under different temperatures.

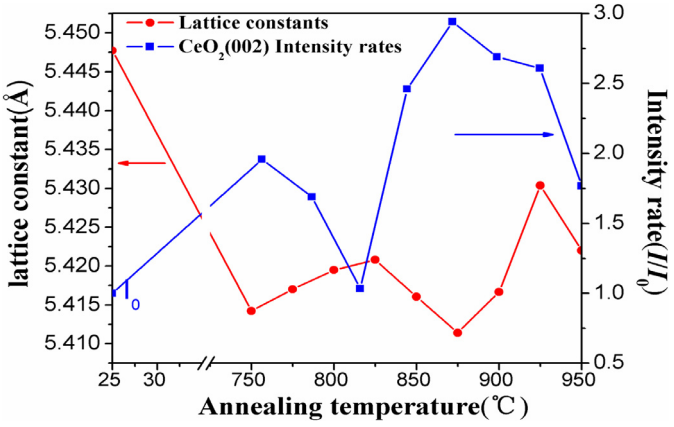

Fig. 2. The dependence of CeO_2 lattice parameters and CeO_2(002)peak intensity with different temperatures.

buffered with Al_2O_3/ Y_2O_3/ IBAD-MgO/ Epi-MgO/ $LaMnO_3$. Cerium oxide template buffers, which annealed at 800 °C is approximately 40 nm thick, were deposited using a large-area magnetron sputtering deposition system on $LaMnO_3$ layers. After deposition, CeO_2 buffers are post-annealed ex-situ at different temperatures. It is found that the crystalline quality of CeO_2 is sensitive to annealing temperature from Fig. 1.

By comparing the influence of different annealing temperatures on lattice parameters and peak intensity of CeO_2, we attempt to manipulate the stabilization process for optimization of annealing temperature region in Fig. 2.

The crystallite size of the films, D, was calculated by Scherrer's formula as:$D = K\lambda/(\beta cos\theta)$,Where $k = 0.9$ is the Scherrer constant, $\lambda = 1.5406$ Å is the wavelength of X-ray diffraction. β is a full width at half maxima of (002) peak, and θ corresponds to the Bragg angle.

Considering both peak shift of $LaMnO_3$(LMO) and lattice constants of CeO_2, we optimized different post-annealing temperatures. The dependence of lattice parameters of CeO_2 peak intensity ratio of CeO_2 on post-annealing temperatures are shown in Fig. 2. As shown in Figs. 1 and 2, no obvious peak shift of $LaMnO_3$(LMO) and excellent crystallinity of CeO_2 is observed for the specimen post-annealed at 875 °C.It was reported that high oxygen partial pressure can decrease the particle energy, posing a hazard for film qualities, but other results argue the variation in oxygen partial pressure has no effect on the crystalline orientation of CeO_2 layers [17]. So we did not pay more attention to it. A significant improvement of CeO_2 crystallinity is obtained for annealing temperature at 875 °C. Thus we fixed post-annealing temperature at 875°Cand turned to varying post-annealing atmospheres. The Cerium oxide are post-annealed for 60 min at 875 °C in various flowing gas [18] as follows: (a) Ar-5%H_2, (b) humid Ar-5%H_2, (c)O_2, with the corresponding samples termed S1,S2,S3 respectively and the specimen without post-annealing is named S0.

Finally the Y(Dy)BCO layers about 1 μm are deposited on the above ceria buffers via a low fluorine metal organic deposition (MOD) process. The synthesize and heat-treatment process for low-fluorine Y(Dy)BCO films have been reported in our previous work [19–21].

The structure and the texture of the grown films of CeO_2 with and without post-annealing are characterized by glancing incidence X-ray diffraction $\theta-2\theta$ scans and ω-scans (Philips X'Pert PRO, CuKα radiation operated at 40 mA and 40 kV). The morphology, valence state, microstructure and size of CeO_2 are evaluated by scanning electron microscopy(SEM), atomic force microscopy(AFM) and X-rays photoelectron spectroscopy(XPS). The spectroscopic measurements of samples are carried out in a ultra-high-vacuum system(5×10^{-8} mbar) with an analysis chamber. And the measurements (here Al Kα irradiation used at an excitation voltage of 14.5 KV and an emission current of 18.15 mA, scan area is 500 μm × 500 μm) scan deeper layer < 10 nm without annealing in XPS chamber. The surface of Y(Dy)BCO profile is tested by metallographic microscope. The J_c of Y(Dy)BCO films were measured at 77 K by an inductive measurement system from Theva. The critical current (I_c) of the coated conductors were obtainned via multiplying critical current density (J_c) by the corresponding cross-sectional area (S).

3. Results and discussion

Comparing with the conventional evaluation system about cap layer, the present mechanism manifests the surface quality and the lattice mismatch with the substrate, or the cap layer in the case of multilayered structures influencing the interfacial nucleation phenomena of Y(Dy)BCO grains strongly [22–26].

In order to distinguish the lattice mismatch with Y(Dy)BCO and surface quality of the post-annealing CeO_2, the post-annealed samples are analyzed by different characterization methods.

Fig. 3 (a–d) show the high-resolution reciprocal space mapping(HR-RSM) of the CeO_2 (002) deposited at different ambient flowing gas. After post-annealed, the surface of buffer layer occurs adsorption and separation reaction with the atoms of different gases. The gas atoms and atoms from surface buffer layer exchange electrons, forming chemical bond. Therefore, the out-of-plane texture of ceria oxide undergoes different changes. The HR-RSM results show that the CeO_2 films post-annealed under different atmosphere exhibit different growth morphology. Fig. 3b and d display broader RSMs range in the 2Theta direction, revealing poorer crystallization of the film post-annealed under such atmosphere. When the CeO_2 layer was post-annealed in the surrounding of humid Ar-5%H_2 gas, the RSMs show a considerably converged pattern in the 2Theta and omega directions, demonstrating humid Ar/5%H_2 gas is suitable for the regrowth of CeO_2 layer on the LMO substrate. Based on the above analysis, the structural optimization of CeO_2 film post-processed in wet Ar/5%H_2 flowing gas overwhelms that of other films. Furthermore, the HR-RSM area of the CeO_2 post-annealed in humid Ar/5%H_2 atmosphere exhibits smallest overall *c*-axis tilts.

The ϕ-scans are carried out to evaluate the in-plane texture of CeO_2 with and without being post-annealed. Four symmetric peaks average full width at half-maximum (FWHM) values about the ϕ-scan patterns are shown in Table 1, indicating all the CeO_2 films have strong biaxial texture. Obviously the structure of S2 is slightly better than other samples and more suitable for subse-